HHS Public Access

Author manuscript

Kidney Int. Author manuscript; available in PMC 2018 July 17.

Published in final edited form as:

Kidney Int. 2011 July ; 80(1): 61–67. doi:10.1038/ki.2011.67.

Decreased bone density and increased phosphaturia in gene-targeted mice lacking functional serum- and glucocorticoid-inducible kinase 3

Madhuri Bhandaru[1], **Daniela S. Kempe**[1], **Anand Rotte**[1], **Paola Capuano**[2], **Ganesh Pathare**[1], **Mentor Sopjani**[1], **Ioana Alesutan**[1], **Leonid Tyan**[1], **Dan Yang Huang**[3], **Balasaheb Siraskar**[1], **Martin S. Judenhofer**[4], **Gerti Stange**[2], **Bernd J. Pichler**[4], **Jürg Biber**[2], **Leticia Quintanilla-Martinez**[5], **Carsten A. Wagner**[2], **David Pearce**[6], **Michael Föller**[1], and **Florian Lang**[1]

[1]Department of Physiology, University of Tübingen, Tübingen, Germany [2]Institute of Physiology and Zurich Center for Integrative Human Physiology, University of Zurich, Zurich, Switzerland [3]Department of Pharmacology and Toxicology, University of Tübingen, Tübingen, Germany [4]Department of Radiology, University of Tübingen, Tübingen, Germany [5]Department of Pathology, University of Tübingen, Tübingen, Germany [6]Department of Medicine (Nephrology), University of California, San Francisco, California, USA

Abstract

Insulin and growth factors activate the phosphatidylinositide-3-kinase pathway, leading to stimulation of several kinases including serum- and glucocorticoid-inducible kinase isoform SGK3, a transport regulating kinase. Here, we explored the contribution of SGK3 to the regulation of renal tubular phosphate transport. Coexpression of SGK3 and sodium-phosphate cotransporter IIa significantly enhanced the phosphate-induced current in *Xenopus* oocytes. In *sgk3* knockout and wild-type mice on a standard diet, fluid intake, glomerular filtration and urine flow rates, and urinary calcium ion excretion were similar. However, fractional urinary phosphate excretion was slightly but significantly larger in the knockout than in wild-type mice. Plasma calcium ion, phosphate concentration, and plasma parathyroid hormone levels were not significantly different between the two genotypes, but plasma calcitriol and fibroblast growth factor 23 concentrations were significantly lower in the knockout than in wild-type mice. Moreover, bone density was significantly lower in the knockouts than in wild-type mice. Histological analysis of the femur did not show any differences in cortical bone but there was slightly less prominent trabecular bone in *sgk3* knockout mice. Thus, SGK3 has a subtle but significant role in the regulation of renal tubular phosphate transport and bone density.

Keywords

calcium; insulin; mineralization; phosphate; PTH; $1,25(OH)_2D_3$

Correspondence: Florian Lang, Department of Physiology, University of Tübingen, Gmelin Street 5, D-72076, Tübingen, Germany., florian.lang@uni-tuebingen.de.

DISCLOSURE

All the authors declared no competing interests.

Phosphate is a critically important component of bone minerals.[1,2] Accordingly, adequate mineralization of bone depends on the precise tuning of phosphate balance, which is a function of intestinal absorption and renal excretion.[1,3,4] The latter depends on cellular uptake of phosphate across the apical membrane of proximal tubular cells,[5] which is mainly accomplished by the Na +-coupled phosphate transporter NaPiIIa.[3,5] The carrier is downregulated by parathyroid hormone (PTH),[3] a hormone at least in part effective through cyclic adenosine monophosphate. In contrast, renal tubular phosphate reabsorption is stimulated by insulin[6,7] and insulin-like growth factor IGF1.[8,9] Little is known, however, about the signaling involved in the insulin- and IGF1-mediated regulation of phosphate excretion.

The signaling of insulin involves the serum- and glucocorticoid-inducible kinase SGK3,[10] which, similar to protein kinase B[11] and SGK1,[12] is activated by phosphatidy-linositol-3-kinase and phosphoinositide-dependent kinase PDK1. SGK3 is known to regulate a wide variety of transport systems.[13]

The present study thus explored the possibility that SGK3 may be involved in the regulation of renal tubular transport. To this end, the *in vitro* regulation of NaPiIIa by SGK3 was studied in the heterologous *Xenopus* oocyte expression system and *in vivo* significance of SGK3-sensitive phosphate transport elucidated by analyzing gene-targeted mice lacking functional SGK3 ($sgk3^{KO}$) as well as wild-type mice ($sgk3^{WT}$).[14]

RESULTS

A first series of experiments analyzed the *in vitro* influence of the serum- and glucocorticoid-inducible kinase isoform SGK3 on NaPiIIa, the major renal tubular phosphate transporter. Exposure of non-injected *Xenopus* oocytes to phosphate (3 mmol/l) in the bath solution did not induce a significant current, indicating that these oocytes do not express significant endogenous electrogenic phosphate transport (Figure 1a). In oocytes injected with complementary RNA encoding NaPiIIa, however, the addition of phosphate (3 mmol/l) induced an inward current (I_{Pi}; Figure 1a). Coexpression of SGK3 significantly increased I_{Pi} in NaPiIIa-expressing oocytes (Figure 1a). Expression of SGK3 alone did not induce I_{Pi}, indicating that SGK3 was indeed effective by stimulating NaPiIIa. The membrane abundance of NaPiIIa in oocytes was determined by a chemiluminiscence-based assay. As shown in Figure 1b, coexpression of SGK3 significantly increased the surface expression of NaPiIIa to a similar extent as it stimulated phosphate-induced currents.

Experiments in brush border membrane vesicle (BBMV) preparations from $sgk3^{KO}$ and $sgk3^{WT}$ mice were performed to determine the sodium-dependent transport of phosphate *ex vivo*. However, no significant difference in total and phosphonoformic acid (6 mmol/l)-resistant transport was observed between $sgk3^{KO}$ and $sgk3^{WT}$ mice (Figure 2). Similarly, the protein expression of the phosphate transporters NaPiIIa, NaPiIIc, and Pit2 in brush border membrane fractions was not different between the genotypes (Figure 2). The transcript levels of these transporters were similarly not significantly different between $sgk3^{KO}$ and $sgk3^{WT}$ mice (data not shown).

A further series of experiments explored whether SGK3 participates in the regulation of renal phosphate excretion *in vivo*. To this end, metabolic cage experiments were performed in $sgk3^{KO}$ and $sgk3^{WT}$ mice. As shown in Table 1, the body weight was similar in $sgk3^{KO}$ mice and $sgk3^{WT}$ mice. Fluid intake tended to be slightly higher in $sgk3^{KO}$ than in $sgk3^{WT}$ mice, a difference, however, not reaching statistical significance (Table 1). Food intake was slightly but significantly higher in $sgk3^{KO}$ than in $sgk3^{WT}$ mice (Table 1).

No significant differences between the genotypes were observed in the plasma Ca^{2+} and phosphate concentration (Table 1, Figure 3). Similarly, the plasma glucose concentration was not significantly different between genotypes (data not shown).

The urinary flow rate and creatinine clearance tended to be slightly higher in $sgk3^{KO}$ mice than in $sgk3^{WT}$ mice, a difference, however, not reaching statistical significance (Table 1). The absolute (Table 1) and fractional (Figure 3) excretions of Ca^{2+} were not significantly different between the two genotypes. In contrast, the absolute (Table 1) and fractional (Figure 3) excretions of phosphate were significantly higher in $sgk3^{KO}$ mice than in $sgk3^{WT}$ mice. In neither the $sgk3^{WT}$ nor the $sgk3^{KO}$ mice, glucosuria was observed (data not shown).

The renal phosphate excretion was further studied under a low-phosphate diet. The urinary phosphate excretion was still significantly higher in $sgk3^{KO}$ (0.17±0.03 μmol/24 h per g body weight; $n = 5$) than in $sgk3^{WT}$ (0.10±0.01 μmol/24 h per g body weight; $n = 6$) mice. To further analyze the renal function of those mice, acute inulin clearance studies were performed under anesthesia. The glomerular filtration rate (GFR) as determined from the inulin clearance was not significantly different between $sgk3^{WT}$ (119±28 μl/min; $n = 5$) and $sgk3^{KO}$ (92±22 μl/min; $n = 5$) mice. In this series, the fractional excretion of phosphate was again higher in $sgk3^{KO}$ (2.4±0.3%) than in $sgk3^{WT}$ (1.7±0.1%) mice.

The phosphaturia could have been secondary to altered levels of hormones involved in phosphate homeostasis. Therefore, the plasma levels of PTH, calcitriol ($1,25(OH)_2D_3$) and fibroblast growth factor 23 (FGF 23) were determined. As illustrated in Figure 4, the PTH plasma concentration was not significantly different between the genotypes, whereas the plasma $1,25(OH)_2D_3$ and plasma FGF23 concentrations were significantly lower in $sgk3^{KO}$ mice compared with $sgk3^{WT}$ mice.

The renal loss of phosphate is expected to foster demineralization of bone. Thus, the bone density was determined in $sgk3^{KO}$ and $sgk3^{WT}$ mice. As shown in Figure 5a, the bone density was indeed lower in $sgk3^{KO}$ than in $sgk3^{WT}$ mice. A histological analysis of the femur showed no obvious differences in the cortical bone between the two genotypes but revealed that the trabecular bone appeared to be less prominent in $sgk3^{KO}$ mice than in $sgk3^{WT}$ mice (Figure 5b).

DISCUSSION

The present observations disclose a novel function of SGK3, that is, stimulation of renal tubular phosphate transport. According to the experiments on *Xenopus* oocytes, coexpression of SGK3 increases NaPiIIa activity. The *in vivo* relevance of SGK3-sensitive NaPiIIa regulation is underscored by the mild phosphaturia of $sgk3^{KO}$ mice.

The phosphaturia of *sgk3*^{KO} mice was not due to an increased plasma phosphate concentration and occurs without significant alterations of the PTH plasma concentration. The hormone is well known to downregulate renal phosphate transport,[3] and its release is stimulated by an enhanced plasma phosphate concentration.[15] The plasma levels of $1,25(OH)_2D_3$ were significantly decreased in *sgk3*^{KO} mice. The rate-limiting enzyme in the generation of $1,25(OH)_2D_3$ is the renal 1α-hydroxylase,[16,17] which is stimulated by PTH[17] and cellular phosphate depletion.[18] A decreased NaPiIIa activity is expected to decrease the entry of phosphate into proximal tubule cells and thus to rather decrease the phosphate concentration in proximal tubular cells. A decreased cellular phosphate concentration is in turn expected to increase the $1,25(OH)_2D_3$ formation. Possibly, SGK3 participates in the regulation of $1,25(OH)_2D_3$ formation, which has previously been shown to be stimulated by IGF1.[19] As $1,25(OH)_2D_3$ stimulates renal tubular phosphate transport,[20] decreased $1,25(OH)_2D_3$ formation could contribute to the phosphaturia of *sgk3*^{KO} mice. Moreover, $1,25(OH)_2D_3$ is a powerful stimulator of intestinal phosphate transport.[21] It is, however, not required for the adaptive increase in intestinal phosphate absorption in dietary phosphate depletion.[22] The decrease of $1,25(OH)_2D_3$ plasma levels may account for the decreased formation of FGF23, which should rather disinhibit 1α-hydroxylase and should thus increase $1,25(OH)_2D_3$ concentrations. The decreased FGF23 levels were expected to counteract renal phosphate losses.

We did not observe a significant decrease of the plasma phosphate concentration despite the mild phosphaturia. Enhanced phosphate excretion must thus be paralleled by enhanced intestinal phosphate absorption or phosphate loss from bone. In an earlier study, fecal phosphate excretion was not significantly different between *SGK3*^{KO} and *sgk3*^{WT} mice.[23] However, the food intake was significantly higher in *sgk3*^{KO} mice than in *sgk3*^{WT} mice, and thus intestinal phosphate absorption might indeed have been increased.

The phosphaturia of *sgk3*^{KO} mice was not paralleled by a decrease of phosphate transport across BBMVs or of mRNA and protein abundance of the phosphate transporters. The lack of significant differences between tissue of *sgk3*^{WT} mice and *sgk3*^{KO} mice is at seeming contrast to the powerful effect of SGK3 on NaPiIIa expression in *Xenopus* oocytes. It must be kept in mind, although, that the *in vivo* effect of SGK3 is paralleled by a similar effect of PKB/Akt,[24] and thus knockout of one of the kinases in mice does not abrogate SGK3/PKB/AKT-dependent regulation of NaPiIIa and is thus not expected to yield similarly strong effects as overexpression of SGK3 in *Xenopus* oocytes. The mild phosphaturia of *sgk3*^{KO} mice confirms that SGK3 indeed participates in the regulation of renal tubular phosphate reabsorption. It remains elusive, although, why the phosphaturia is not reflected by respective alterations of carrier protein abundance and phosphate uptake in brush border vesicles. Possibly, SGK3 does not only affect NaPiIIa abundance in a heterologous expression system such as oocytes, but may also stimulate the activity of phosphate transporter *in vivo* without altering their cell surface expression.

The *sgk3*^{KO} mice suffer from a subtle but significant decrease of bone mass, which may again be partially due to decreased formation of $1,25(OH)_2D_3$. The $1,25(OH)_2D_3$ is known to counteract apoptosis of osteoblasts[25] and thus enhances bone mineralization.[26] The effect of $1,25(OH)_2D_3$ in osteoblasts is mediated by the phosphoinositide-3-kinase pathway,[27] and

may thus involve at least partially SGK3. The demineralization of bone may further be due to phosphate depletion, as phosphate inhibits the formation of new osteoclasts and stimulates apoptosis of mature osteoclasts.[28] The present observations do not rule out the participation of further mechanisms. For instance, SGK3 shares several functions with Akt2/PKBβ,[29] which has been shown to confer survival of osteoblasts[30] and osteoclasts.[31,32]

In conclusion, the present observations reveal a novel function of SGK3, that is, its involvement in the regulation of $1,25(OH)_2D_3$ plasma concentration, renal phosphate excretion, and mineralization of bone.

MATERIALS AND METHODS

In vitro experiments

For generation of complementary RNA, constructs were used encoding wild-type human NaPiIIa[33] and human SGK3.[10] The complementary RNA was generated as described previously.[34] SGK3 cDNA was kindly provided by Sir Philip Cohen (MRC Protein Phosphorylation Unit, Dundee) and the cDNA encoding NaPiIIa by Heini Murer, (University of Zurich, Zurich). For electrophysiology, *Xenopus* oocytes were prepared as previously described.[35,36] Wild-type SGK3 (7.5 ng) and 15 ng of NaPiIIa complementary RNA were injected on the same day after preparation of *Xenopus* oocytes. All experiments were performed at room temperature 4–5 days after injection. Two electrode voltage-clamp recordings were performed at a holding potential of −50 mV.[37] The data were filtered at 10 Hz and recorded with a Digidata A/D-D/A converter and Chart V.4.2 software for data acquisition and analysis (Axon Instruments, Berlin, Germany).[38] The control solution (superfusate/ND96) contained 96 mmol/l NaCl, 2 mmol/l KCl, 1.8 mmol/l $CaCl_2$, 1 mmol/l $MgCl_2$, and 5 mmol/l HEPES, pH 7.4. Phosphate (2 mmol/l) was added to induce NaPiIIa-dependent currents. The flow rate of the superfusion was 20 ml/min, and a complete exchange of the bath solution was reached within about 10 s. All experiments were repeated with at least three batches of oocytes; in all repetitions, qualitatively similar data were obtained.

Detection of NaPilla cell surface expression by chemiluminescence

Defolliculated oocytes were incubated with primary rabbit anti-NaPiIIa antibody (diluted 1:500, Lifespan Biosciences, Seattle, WA) and secondary, peroxidase-conjugated goat anti-rabbit antibody (diluted 1:1000, Cell Signaling, Danvers, MA). Individual oocytes were placed in 96-well plates with 10 μl of Super Signal ELISA Femto Maximum Sensitivity Substrate (Pierce, Rockford, IL). Chemiluminescence of single oocytes was quantified in a luminometer (WalterWallac2 plate reader, Perkin Elmer, Jügesheim, Germany) by integrating the signal over a period of 1 s. Results display normalized arbitrary light units that are proportional to the detector voltage.

In vivo function

All animal experiments were conducted according to the German law for the welfare of animals and were approved by local authorities.

Generation and basic properties of the SGK3 knockout mice ($sgk3^{KO}$) were described previously.[39] The mice were compared with the wild-type mice ($sgk3^{WT}$) and genotyped by PCR on tail DNA using SGK3- and neoR-specific primers as previously described.[39]

The mice (age 3.5–6 months) were fed a control diet containing 0.7% phosphate (C1314, Altromin, Lage, Germany) or 7-day-low-phosphate diet containing less than 0.1% phosphate (C 1048 Altromin, Germany) with free access to tap drinking water.

For evaluation of renal excretion, both $sgk3^{KO}$ and $sgk3^{WT}$ mice were placed individually in metabolic cages (Techniplast, Hohenpeissenberg, Germany) for 24-h urine collection, as described previously.[40] They were allowed a 3-day habituation period during which food and water intake, urinary flow rate, urinary excretion of salt, fecal excretion, and body weight were recorded every day to ascertain that the mice were adapted to the new environment. Subsequently, 24-h collection of urine was performed for several consecutive days to obtain the urinary parameters. To assure quantitative urine collection, metabolic cages were siliconized, and urine was collected under water-saturated oil.

To obtain blood specimens, animals were lightly anesthetized with diethylether (Roth, Karlsruhe, Germany), and about 150 µl of blood was withdrawn into heparinized capillaries by puncturing the retro-orbital plexus.

Urinary phosphate concentration was determined colorimetrically utilizing a commercial diagnostic kit (Roche Diagnostics, Mannheim, Germany). Plasma and urinary calcium, and plasma phosphate concentration were determined by a photometric method according to the manufacturer's instructions (drichem clinical chemistry analyzer FUJI FDC 3500i, Sysmex, Norsted, Germany). Creatinine concentration in urine was determined using the Jaffe reaction (Sigma, St Louis, MO), creatinine concentration in serum was measured using an enzymatic kit (creatinine PAP, Lehmann, Berlin, Germany) according to the manufacturer's instructions. Plasma PTH concentration was measured using an ELISA kit (Immunotopics, San Clemente, CA). A radioimmunoassay kit was employed to determine the concentration of $1,25(OH)_2$-vitamin D_3 (IDS, Boldon, UK) in plasma. Plasma FGF23 was determined using an ELISA kit (Immunotopics, San Clemente, CA).

Clearance experiments

Clearance experiments were performed in anaesthetized SGK3 wild-type and knockout mice ($n = 5$ in each group), as described previously.[41,42] Briefly, mice were anesthetized intraperitoneally with 80 mg/kg sodium pentobarbital. Body temperature was maintained at 37.5 °C by placing the animals on an operating table with a servo-controlled heating plate. The trachea was cannulated for free air breathing throughout the experiment. The left femoral artery was cannulated for arterial blood pressure recording and blood sample withdrawal. The right jugular vein was cannulated for continuous maintenance infusion of 0.85% NaCl at a rate of 8 µl/min. For assessment of GFR, [3H]-inulin was added into 0.85% NaCl solution to deliver 20 µCi/h radioactive inulin. Urine samples were collected via a catheter inserted into the urinary bladder. After surgical preparation, mice were allowed to stabilize for 20 min. Subsequently, to determine renal function, a 60-min urine collection period was performed. Blood samples (80 µl) were collected immediately before and after

urine collections. Blood pressure was recorded before every blood sample collection. Urinary flow rate was determined gravimetrically. Concentrations of [3H]inulin in plasma and urine were measured by liquid-phase scintillation counting. The glomerular filtration rate was calculated according to standard formulas.

Brush border membrane preparation and phosphate transport assays

BBMVs were prepared from mice kidney cortex and outer medulla using the Mg^{2+} precipitation technique, as described previously.[43] The phosphate transport rate into BBMVs was measured in freshly prepared BBMV at 25 °C in the presence of inward gradients of 100 mmol/l NaCl or 100 mmol/l KCl and 0.1 mmol/l K phosphate. The substrate inorganic phosphate was made with 0.125 mmol/l K_2HPO_4 and ^{32}P (1 μCi/ml) to yield a final concentration 0.1 mmol/ l close to the expected apparent KmPi for Na^+-dependent transport in renal BBMVs. The stop solution contained 100 mmol/l mannitol, 5 mmol/l Tris-HCl, pH 7.4, 150 mmol/l NaCl, and 5 mmol/l inorganic phosphate. Na^+ dependence was established by incubating BBMVs in solutions in which KCl replaced NaCl equimolarly. Phosphate uptake was determined after 60 s, representing initial linear conditions, and after 120 min, to determine the equilibrium values. To distinguish between Na^+-dependent inorganic phosphate uptake mediated by SLC34 family members (for example, NaPiIIa and NaPiIIc) and other Na^+-dependent phosphate transporters, such as SLC20 family members (for example, Pit1 and Pit2), trisodium phosphonoformic acid (final concentration 6 mmol/l) added to the same solution with 107 mmol/l NaCl was used. Phosphonoformic acid has previously been shown to have a higher selectivity for SLC34 than SLC20 phosphate transporters at this concentration.[44] The total protein concentration was measured using the Bio-Rad Protein Assay kit; Bio-Rad, Hercules, CA. BBMVs were stored at −80 °C until further use.

Western blotting

After measurement of the protein concentration (Bio-Rad), 10 μg of renal brush border membrane proteins was solubilized in loading buffer containing dithiothreitol and separated on 8% polyacrylamide gels. For immunoblotting, the proteins were transferred electrophoretically to polyvinylidene fluoride membranes (Immobilon-P, Millipore, Bedford, MA). After blocking with 5% milk powder in Tris-buffered saline/0.1% Tween-20 for 60 min, the blots were incubated with the primary antibodies: rabbit polyclonal anti-NaPiIIa (1:6000)[45] rabbit polyclonal anti-NaPiIIc (1:10,000),[46] rabbit polyclonal anti-Pit2 (1:3000; kindly provided by Dr V Sorribas, University of Zaragosa, Spain),[44] and mouse monoclonal anti-β-actin antibody (42 kD; Sigma; 1:5000) either for 2 h at room temperature or overnight at 4 °C. Membranes were then incubated for 1 h at room temperature with secondary goat anti-rabbit or donkey anti-mouse antibodies (1:5000) linked to alkaline phosphatase (Promega, Madison, WI) or HRP (Amersham, Freiburg, Germany). The protein signal was detected with the appropriate substrates (Millipore) using the DIANA III-chemiluminescence detection system (Raytest, Straubenhardt, Germany). All images were analyzed using the software Advanced Image Data Analyser AIDA (Raytest) to calculate the protein of interest/β-actin ratio.

Determination of bone density

For the analysis of bone density, animals were killed and hind legs were removed and fixed in formalin. The samples were scanned with a high-resolution microCAT-II (Siemens, München, Germany) small-animal-computed tomography scanner using a field of view of $3.1 \times 3.1 \times 4.8\ cm^3$. The X-ray tube parameters were set at 80 kVp and 400 μA. The images were acquired with 720 angular projections (exposure time 1200 ms per projection) over 360° and binned with a factor of two, yielding a spatial resolution of ~38 μm. The total scan time was 24 min. Reconstructed computed tomography images were analyzed with the Inveon Research Workplace software (Siemens) by drawing a standard-sized area around the femur and applying a region growth routine to segment the trabecular bone structure. For all samples, the same upper- and lower-density thresholds were applied comparing the relative numbers of trabecular bone density.

Bone histology

For morphological bone analysis, femurs of $sgk3^{KO}$ and $sgk3^{WT}$ mice ($n = 5–6$ in each group) were fixed in 4.5% buffered formalin (Roti-Histofix 4.5%, Roth, Karlsruhe, Germany) for at least 24 h. Decalcification was performed in EDTA solution at room temperature for 2–3 days. The decalcified bones were embedded in paraffin and cut in 2- to 3-μm thick sections and stained with hematoxylin and eosin.

Statistical analysis

Data are provided as arithmetic means±s.e.m., n represents the number of independent experiments. All data were tested for significance using analysis of variance (Figure 1) or paired or unpaired Student's t-test. Only results with $P<0.05$ were considered statistically significant.

Acknowledgments

We acknowledge the technical assistance of Elfriede Faber and Daniel Bukala, as well as the meticulous preparation of the manuscript by Lejla Subasic. This study was supported by the Deutsche Forschungsgemeinschaft, Nr La 315/4-3 and La 315/6-1, and the Swiss National Science Foundation (3100A0-122217).

References

1. Berndt T, Kumar R. Phosphatonins and the regulation of phosphate homeostasis. Annu Rev Physiol. 2007; 69:341–359. [PubMed: 17002592]
2. Liu S, Quarles LD. How fibroblast growth factor 23 works. J Am Soc Nephrol. 2007; 18:1637–1647. [PubMed: 17494882]
3. Murer H, Hernando N, Forster I, et al. Proximal tubular phosphate reabsorption: molecular mechanisms. Physiol Rev. 2000; 80:1373–1409. [PubMed: 11015617]
4. Takeda E, Taketani Y, Sawada N, et al. The regulation and function of phosphate in the human body. Biofactors. 2004; 21:345–355. [PubMed: 15630224]
5. Forster IC, Hernando N, Biber J, et al. Proximal tubular handling of phosphate: a molecular perspective. Kidney Int. 2006; 70:1548–1559. [PubMed: 16955105]
6. Allon M. Effects of insulin and glucose on renal phosphate reabsorption: interactions with dietary phosphate. J Am Soc Nephrol. 1992; 2:1593–1600. [PubMed: 1610980]
7. DeFronzo RA, Goldberg M, Agus ZS. The effects of glucose and insulin on renal electrolyte transport. J Clin Invest. 1976; 58:83–90. [PubMed: 932211]

8. Feld S, Hirschberg R. Insulinlike growth factor I and the kidney. Trends Endocrinol Metab. 1996; 7:85–93. [PubMed: 18406731]
9. Jehle AW, Forgo J, Biber J, et al. IGF-I and vanadate stimulate Na/Pi-cotransport in OK cells by increasing type II Na/Pi-cotransporter protein stability. Pflugers Arch. 1998; 437:149–154. [PubMed: 9817799]
10. Kobayashi T, Deak M, Morrice N, et al. Characterization of the structure and regulation of two novel isoforms of serum- and glucocorticoid-induced protein kinase. Biochem J. 1999; 344(Part 1):189–197. [PubMed: 10548550]
11. Alessi DR, Andjelkovic M, Caudwell B, et al. Mechanism of activation of protein kinase B by insulin and IGF-1. EMBO J. 1996; 15:6541–6551. [PubMed: 8978681]
12. Kobayashi T, Cohen P. Activation of serum- and glucocorticoid-regulated protein kinase by agonists that activate phosphatidylinositide 3-kinase is mediated by 3-phosphoinositide-dependent protein kinase-1 (PDK1) and PDK2. Biochem J. 1999; 339(Part 2):319–328. [PubMed: 10191262]
13. Lang F, Bohmer C, Palmada M, et al. (Patho)physiological significance of the serum- and glucocorticoid-inducible kinase isoforms. Physiol Rev. 2006; 86:1151–1178. [PubMed: 17015487]
14. McManus EJ, Sakamoto K, Armit LJ, et al. Role that phosphorylation of GSK3 plays in insulin and Wnt signalling defined by knockin analysis. EMBO J. 2005; 24:1571–1583. [PubMed: 15791206]
15. Martin DR, Ritter CS, Slatopolsky E, et al. Acute regulation of parathyroid hormone by dietary phosphate. Am J Physiol Endocrinol Metab. 2005; 289:E729–E734. [PubMed: 15914507]
16. Kato S. Genetic mutation in the human 25-hydroxyvitamin D3 1alpha-hydroxylase gene causes vitamin D-dependent rickets type I. Mol Cell Endocrinol. 1999; 156:7–12. [PubMed: 10612418]
17. Portale AA, Miller WL. Human 25-hydroxyvitamin D-1alpha-hydroxylase: cloning, mutations, and gene expression. Pediatr Nephrol. 2000; 14:620–625. [PubMed: 10912530]
18. Perwad F, Azam N, Zhang MY, et al. Dietary and serum phosphorus regulate fibroblast growth factor 23 expression and 1,25-dihydroxyvitamin D metabolism in mice. Endocrinology. 2005; 146:5358–5364. [PubMed: 16123154]
19. Menaa C, Vrtovsnik F, Friedlander G, et al. Insulin-like growth factor I, a unique calcium-dependent stimulator of 1,25-dihydroxyvitamin D3 production. Studies in cultured mouse kidney cells. J Biol Chem. 1995; 270:25461–25467. [PubMed: 7592714]
20. Kurnik BR, Huskey M, Hruska KA. 1,25-Dihydroxycholecalciferol stimulates renal phosphate transport by directly altering membrane phosphatidylcholine composition. Biochim Biophys Acta. 1987; 917:81–85. [PubMed: 3790614]
21. Brown AJ, Finch J, Slatopolsky E. Differential effects of 19-nor-1,25-dihydroxyvitamin D(2) and 1,25-dihydroxyvitamin D(3) on intestinal calcium and phosphate transport. J Lab Clin Med. 2002; 139:279–284. [PubMed: 12032488]
22. Capuano P, Radanovic T, Wagner CA, et al. Intestinal and renal adaptation to a low-Pi diet of type II NaPi cotransporters in vitamin D receptor- and 1alphaOHase-deficient mice. Am J Physiol Cell Physiol. 2005; 288:C429–C434. [PubMed: 15643054]
23. Sandu C, Rexhepaj R, Grahammer F, et al. Decreased intestinal glucose transport in the sgk3-knockout mouse. Pflugers Arch. 2005; 451:437–444. [PubMed: 15971077]
24. Kempe DS, Ackermann TF, Boini KM, et al. Akt2/PKBbeta-sensitive regulation of renal phosphate transport. Acta Physiol (Oxf). 2010; 200:75–85. [PubMed: 20236253]
25. Morales O, Samuelsson MK, Lindgren U, et al. Effects of 1alpha,25-dihydroxyvitamin D3 and growth hormone on apoptosis and proliferation in UMR 106 osteoblast-like cells. Endocrinology. 2004; 145:87–94. [PubMed: 14525911]
26. van Driel M, Pols HA, van Leeuwen JP. Osteoblast differentiation and control by vitamin D and vitamin D metabolites. Curr Pharm Des. 2004; 10:2535–2555. [PubMed: 15320744]
27. Zhang X, Zanello LP. Vitamin D receptor-dependent 1 alpha,25(OH)2 vitamin D3-induced anti-apoptotic PI3K/AKT signaling in osteoblasts. J Bone Miner Res. 2008; 23:1238–1248. [PubMed: 18410228]
28. Kanatani M, Sugimoto T, Kano J, et al. Effect of high phosphate concentration on osteoclast differentiation as well as bone-resorbing activity. J Cell Physiol. 2003; 196:180–189. [PubMed: 12767054]

29. Lang F, Cohen P. Regulation and physiological roles of serum- and glucocorticoid-induced protein kinase isoforms. Sci STKE. 2001; 2001:RE17. [PubMed: 11707620]
30. Chaudhary LR, Hruska KA. The cell survival signal Akt is differentially activated by PDGF-BB, EGF, and FGF-2 in osteoblastic cells. J Cell Biochem. 2001; 81:304–311. [PubMed: 11241670]
31. Kwak HB, Sun HM, Ha H, et al. AG490, a Jak2-specific inhibitor, induces osteoclast survival by activating the Akt and ERK signaling pathway. Mol Cells. 2008; 26:436–442. [PubMed: 18695355]
32. Lee SE, Chung WJ, Kwak HB, et al. Tumor necrosis factor-alpha supports the survival of osteoclasts through the activation of Akt and ERK. J Biol Chem. 2001; 276:49343–49349. [PubMed: 11675379]
33. Busch AE, Wagner CA, Schuster A, et al. Properties of electrogenic Pi transport by a human renal brush border Na+/Pi transporter. J Am Soc Nephrol. 1995; 6:1547–1551. [PubMed: 8749679]
34. Henrion U, Strutz-Seebohm N, Duszenko M, et al. Long QT syndrome-associated mutations in the voltage sensor of I(Ks) channels. Cell Physiol Biochem. 2009; 24:11–16. [PubMed: 19590188]
35. Boehmer C, Palmada M, Klaus F, et al. The peptide transporter PEPT2 is targeted by the protein kinase SGK1 and the scaffold protein NHERF2. Cell Physiol Biochem. 2008; 22:705–714. [PubMed: 19088452]
36. Boehmer C, Laufer J, Jeyaraj S, et al. Modulation of the voltage-gated potassium channel Kv1. 5 by the SGK1 protein kinase involves inhibition of channel ubiquitination. Cell Physiol Biochem. 2008; 22:591–600. [PubMed: 19088441]
37. Laufer J, Boehmer C, Jeyaraj S, et al. The C-terminal PDZ-binding motif in the Kv1. 5 potassium channel governs its modulation by the Na+/H+ exchanger regulatory factor 2. Cell Physiol Biochem. 2009; 23:25–36. [PubMed: 19255497]
38. Gehring EM, Zurn A, Klaus F, et al. Regulation of the glutamate transporter EAAT2 by PIKfyve. Cell Physiol Biochem. 2009; 24:361–368. [PubMed: 19910676]
39. McCormick JA, Feng Y, Dawson K, et al. Targeted disruption of the protein kinase SGK3/CISK impairs postnatal hair follicle development. Mol Biol Cell. 2004; 15:4278–4288. [PubMed: 15240817]
40. Vallon V. *In vivo* studies of the genetically modified mouse kidney. Nephron Physiol. 2003; 94:1–5.
41. Huang DY, Wulff P, Volkl H, et al. Impaired regulation of renal K+ elimination in the sgk1-knockout mouse. J Am Soc Nephrol. 2004; 15:885–891. [PubMed: 15034090]
42. Huang DY, Vallon V, Zimmermann H, et al. Ecto-5′-nucleotidase (cd73)-dependent and -independent generation of adenosine participates in the mediation of tubuloglomerular feedback *in vivo*. Am J Physiol Renal Physiol. 2006; 291:F282–F288. [PubMed: 16525161]
43. Biber J, Stieger B, Stange G, et al. Isolation of renal proximal tubular brush-border membranes. Nat Protoc. 2007; 2:1356–1359. [PubMed: 17545973]
44. Villa-Bellosta R, Ravera S, Sorribas V, et al. The Na+-Pi cotransporter PiT-2 (SLC20A2) is expressed in the apical membrane of rat renal proximal tubules and regulated by dietary Pi. Am J Physiol Renal Physiol. 2009; 296:F691–F699. [PubMed: 19073637]
45. Custer M, Lotscher M, Biber J, et al. Expression of Na-P(i) cotransport in rat kidney: localization by RT-PCR and immunohistochemistry. Am J Physiol. 1994; 266:F767–F774. [PubMed: 7515582]
46. Nowik M, Picard N, Stange G, et al. Renal phosphaturia during metabolic acidosis revisited: molecular mechanisms for decreased renal phosphate reabsorption. Pflugers Arch. 2008; 457:539–549. [PubMed: 18535837]

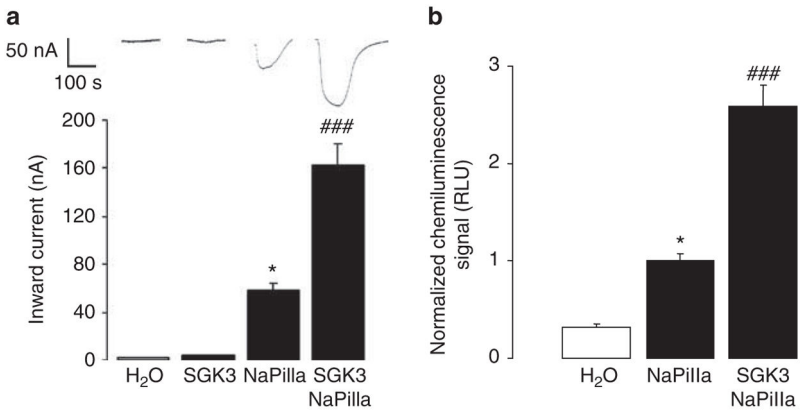

Figure 1. Coexpression of SGK3 stimulates electrogenic phosphate transport in NaPiIIa-expressing *Xenopus* oocytes

(**a**) Arithmetic means±s.e.m. (n = 11–18) of phosphate (3 mmol/l)-induced currents (I_{Pi}) in *Xenopus* oocytes injected with water (H_2O) or complementary RNA (cRNA) encoding SGK3 or NaPiIIa, or cRNA encoding both SGK3 and NaPiIIa. *Indicates significant difference from absence of cRNA encoding NaPiIIa (p<0.05). ###Indicates significant difference from absence of cRNA encoding SGK3 (P<0.001). (**b**) Arithmetic means±s.e.m. (n = 42–60) of the normalized chemiluminescence intensity of NaPiIIa expression in *Xenopus* oocytes injected with H_2O (left bar), with cRNA encoding (middle bar), or with cRNA encoding both, NaPiIIa and SGK3 (right bar). *Indicates statistically significant difference from absence of cRNA (P<0.05). ###Indicates difference from absence of SGK3 cRNA (P<0.001). RLU, relative luminescence.

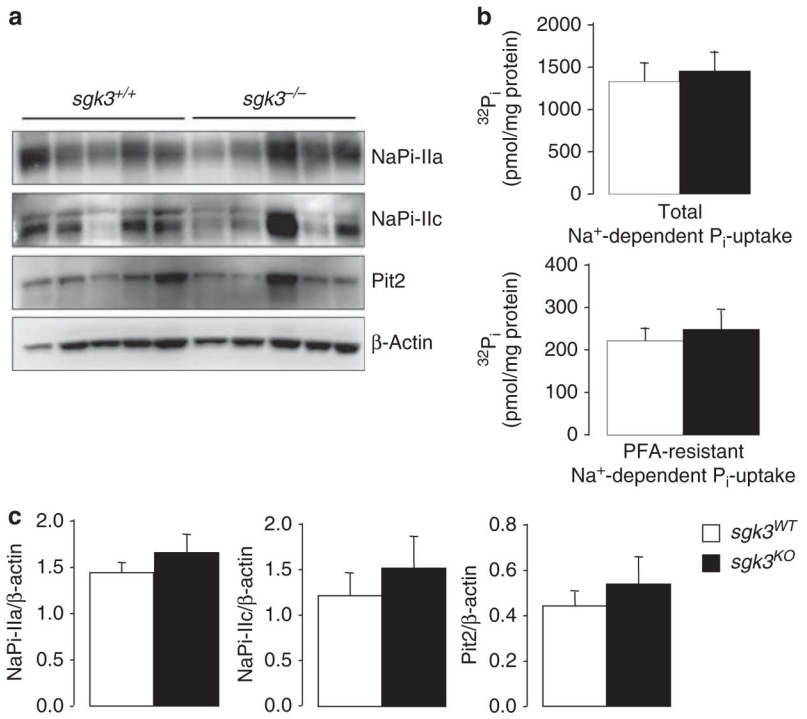

Figure 2. Protein abundance of renal sodium-dependent phosphate cotransporters and sodium-dependent phosphate transport activity in brush border membrane vesicles (BBMVs) of SGK3 knockout mice (*sgk3*^{KO}) and wild-type mice (*sgk3*^{WT}) mice

(**a**) Original western blots for NaPiIIa, NaPiIIc, and Pit2. All membranes were stripped and reprobed for β-actin to control for loading. (**b**) Arithmetic means±s.e.m. (n = 5–6 each group) of the sodium-dependent transport rates into isolated BBMVs after 1 min in the absence (upper bars) and presence (lower bars) of 6 mmol/l phosphonoformic acid (PFA) to block phosphate transport mediated by SLC34 family members. (**c**) Arithmetic means ±s.e.m. (n = 6 each group) of relative band density of NaPilla (left panel), NaPillc (middle panel), and Pit2 (right panel).

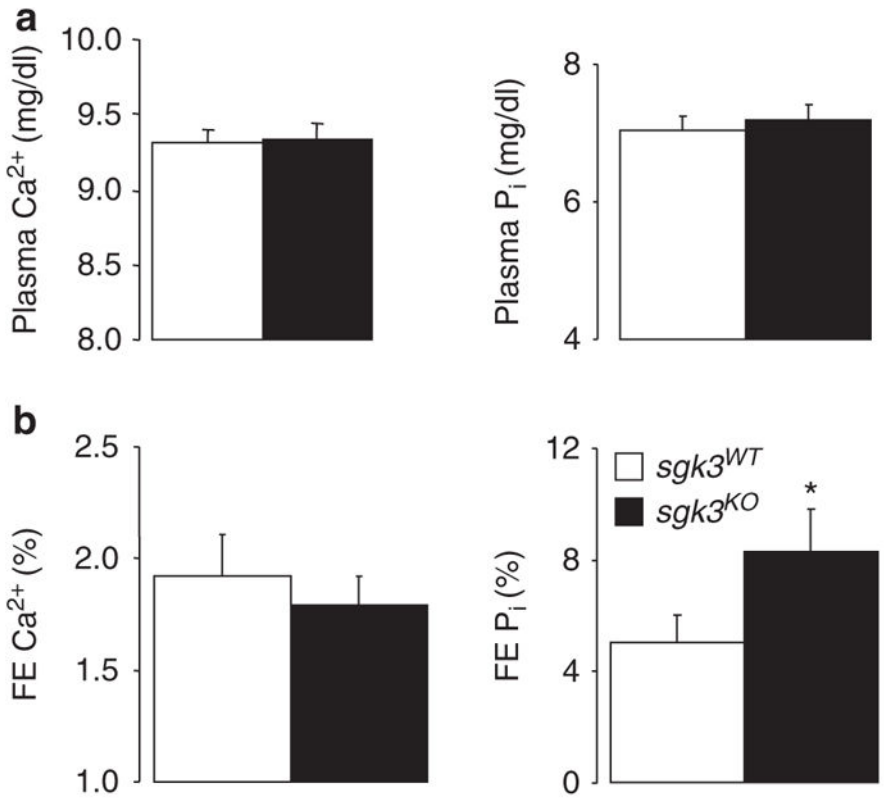

Figure 3. Fractional excretion of calcium and phosphate in SGK3 knockout mice (*sgk3*^{KO}) and wild-type mice (*sgk3*^{WT})

(**a**) Arithmetic means±s.e.m. (n = 10–19 each group) of plasma calcium (left panel) and phosphate (right panel) concentration in *sgk3*^{KO} (closed bars) and *sgk3*^{WT} (open bars) mice. (**b**) Arithmetic means±s.e.m. (n = 10–19 each group) of fractional urinary calcium (left panel) and phosphate (right panel) excretion in *sgk3*^{KO} (closed bars) and *sgk3*^{WT} (open bars) mice. *P<0.05 versus respective value of *sgk3*^{WT} mice. FE, fractional excretion.

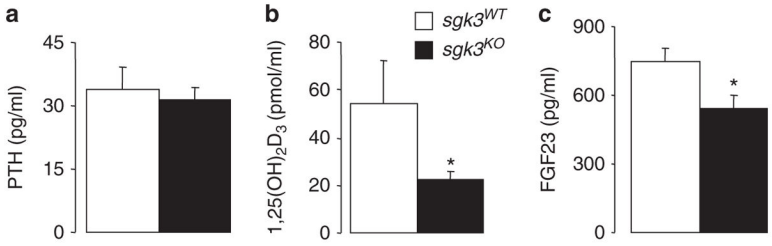

Figure 4. Plasma parathyroid hormone (PTH), FGF23, and calcitriol ($1,25(OH)_2D_3$) concentrations in SGK3 knockout mice ($sgk3^{KO}$) and wild-type mice ($sgk3^{WT}$)

Arithmetic means±s.e.m. of plasma PTH (**a**; n = 10–12 each group), 10 each group), $1,25(OH)_2D_3$ (**b**; n = and FGF23 (**c**; n = 8 in each group) concentration in $sgk3^{KO}$ (closed bars) and $sgk3^{WT}$ (open bars) mice. *P<0.05 versus respective value of $sgk3^{WT}$ mice.

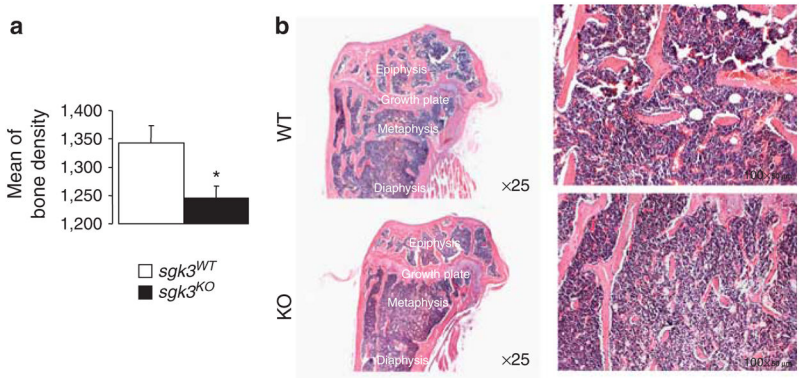

Figure 5. Bone density and histological analysis of femur bones from SGK3 knockout mice (*sgk3*^{KO}) and wild-type mice (*sgk3*^{WT})

(**a**) Arithmetic means±s.e.m. (n = 6 each group) of bone density in *sgk3*^{KO} (closed bar) and *sgk3*^{WT} (open bar) mice. *P<0.05 versus respective value of *sgk3*^{WT} mice. (**b**) Histology of bone in the *sgk3*^{KO} and *sgk3*^{WT} mice representative for n = 5–6 mice each group. The cortical bone is similar but the trabecular bone is less prominent in *sgk3*^{KO} than in *sgk3*^{WT} mice.

Table 1

Analysis of blood and urine of *sgk3*^{KO} and *sgk3*^{WT} mice

	***sgk3*^{WT}**	***sgk3*^{KO}**
BW (g)	23.8±0.6	23.6±0.6
Food intake (mg/g BW)	187±7	207±6 *
Fluid intake (mg/g BW)	275±15	304±16
[Ca^{2+}]plasma (mg/dl)	9.31±0.08	9.33±0.11
[P_i]plasma (mg/dl)	7.04±0.21	7.18±0.22
Urine Ca^{2+} (μmol/24 h per g BW)	0.30±0.02	0.31±0.03
Urine P_i (μmol/24 h per g BW)	0.50±0.12	0.97±0.18 *
Urinary flow rate (μl/24 h per g BW)	48.5±6.3	61.1±5.7
Creatinine clearance (μl/min per g BW)	4.8±0.6	6.1±0.9
Fractional renal Ca^{2+} excretion (%)	1.9±0.2	1.8±0.1
Fractional renal P_i excretion (%)	4.6±0.9	7.6±1.4 *

Abbreviations: BW, body weight; P_i, inorganic phosphate; *sgk3*^{KO}, SGK3 knockout mice; *sgk3*^{WT}, wild-type mice.

BW, food and fluid intake, plasma concentration and renal excretion of Ca^{2+} and phosphate, urinary flow rate, creatinine clearance, and fractional renal excretion of Ca^{2+} and phosphate in *sgk3*^{KO} and *sgk3*^{WT} mice. Arithmetic means ± s.e.m. (n=10–19 mice);

* indicates significant difference between genotypes (P<0.05).